

Article

# Capillary Water Absorption and Micro Pore Connectivity of Concrete with Fractal Analysis

Xiangqun Ding<sup>1</sup>, Xinyu Liang<sup>1</sup>, Yichao Zhang<sup>2,\*</sup>, Yanfeng Fang<sup>1</sup>, Jinghai Zhou<sup>2</sup> and Tianbei Kang<sup>2</sup>

<sup>1</sup> School of Materials Science and Engineering, Shenyang Jianzhu University, Shenyang 110168, China; dingxiangqun@sjzu.edu.cn (X.D.); lunwenww@sina.com (X.L.); fangyf@sjzu.edu.cn (Y.F.)

<sup>2</sup> School of Civil Engineering, Shenyang Jianzhu University, Shenyang 110168, China; zhousinghai@sjzu.edu.cn (J.Z.); kangtianbei@sjzu.edu.cn (T.K.)

\* Correspondence: zhangyichao@sjzu.edu.cn

Received: 28 July 2020; Accepted: 28 September 2020; Published: 1 October 2020



**Abstract:** This study focuses on the relationship between the complexity of pore structure and capillary water absorption of concrete, as well as the connection behavior of concrete in specific directions. In this paper, the water absorption of concrete with different binders was tested during the curing process, and the pore structure of concrete was investigated by mercury intrusion porosimetry (MIP). The results show that the water absorption of concrete with mineral admixtures is lower, mainly due to the existence of reasonable pore structure. The effect of slag on concrete modification is more remarkable comparing with fly ash. In addition, the analysis shows that the pore with different diameters has different fractal characteristics. The connectivity probability and water absorption of unidirectional chaotic pore are linearly correlated with the pore diameter of 50–550 nm, and the correlation coefficient reaches a very significant level, and detailed analysis was undertaken to interpret these results based on fractal theory.

**Keywords:** concrete; pore structure; water absorption; MIP; fractal dimension; pore connectivity

## 1. Introduction

As one of the most commonly used building materials, concrete is inevitably subjected to various destructive factors, which stem from the production process or use environment of concrete. In addition, water is the most common substance accompanied by concrete, which always affects the durability of concrete [1,2]. Harmful ions dissolved in water (e.g., chloride ions, sulfate ions, or magnesium ions) are transported among the complex and disordered pores [3]. Both theoretical and experimental results show that the capillary suction of unsaturated concrete absorbs chloride ions in water and accelerates the corrosion of reinforced concrete under the condition of wetting and drying alternation.

Additionally, sulfate attack also depends on the moisture entering concrete during the process of water transport [4–6]. Water penetrating in and out actually exists in all the processes of deterioration resulting from the freeze-thaw cycle, and the damage extent of concrete shows an ultra-superposition effect under the alternation of wetting and drying [7]. Obviously, water absorption behavior plays an important role in durability of concrete.

The rate at which water is absorbed into concrete by capillary suction can provide useful information relating to the pore structure, the permeation characteristics, and the durability of concrete surface zone [8,9]. Meanwhile, the pore structure of concrete is of great significance to the durability of the material, and the complexity of pore structure has a significant impact on the permeability. The pore size of concrete varies from nanometer scales to micrometer scales, and the pore morphology shown by scanning electron microscopy (SEM) is rather complex and disordered [10].

Fractal theory, as a rising nonlinear science, may solve the problem of evaluating the complexity or roughness of self-similar or approximate self-similar objects effectively. The mathematical beauty of fractal is that it forms the infinite complexity with relatively simple equations and different information captured by test equipment and different definitions of fractal dimension (including the Hausdorff dimension, the box-counting dimension, etc.) [11,12]. Fractal theory has been applied to the study of concrete, and some valuable results have been obtained, especially in pore research, pore fractal dimension. It has a close relationship with the transport performance (chloride diffusion coefficient, depth of carbonation, etc.) as a parameter of the complex transport channel [13,14], which can be used as an index of pore structure damage [15,16]. If it is assumed that the pore can move by itself, the connecting behavior between the pore is a revolution from complexity to simplicity, so it can be inferred that the fractal dimension of the pore and the possibility of the connection correspond to each other. Microstructure parameters measured by MIP and X-ray CT images with different voxel sizes were compared [17].

Fractal theory can better characterize the connectivity of pores. At present, there are few studies on quantitative analysis of pore connectivity by fractal theory. In this study, concrete specimens with different pore structures were prepared by adding different mineral admixtures. In order to obtain the relationship between the complexity of pore structure and the absorption capillary water in specific directions, a series of tests were carried out on the properties of concrete specimens, and the experimental results were compared and discussed by processing data obtained from the test of water absorption and MIP. Finally, fractal theory is used to analyze the relationship of the pore connectivity and water absorption.

## 2. Materials and Mixture Proportions

The 32.5 R ordinary Portland cement was used which is produced by Shenyang Jidong Cement Company, China. The physical properties of cement are shown in Table 1. Additionally, the chemical compositions of fly ash and slag are shown in Table 2. There are three specimens in each group. If the deviation of the test results of three specimens in each group is within 5%, the test results are considered to be valid, and the average value of the test results of the three specimens is taken as the final test results. All experimental results in this paper are based on this method.

Table 1. Physical properties of cement.

80 um Sieve Reside/%	Setting Time/Min		Soundness	Tensile Strength/MPa		Compressive Strength/MPa	
	Initial	Final		3d	28d	3d	28d
1.4	160	220	Qualified	3.3	7.0	16.5	38.1

Table 2. Chemical composition of fly ash and slag (%).

Chemical Composition	SiO <sub>2</sub>	Al <sub>2</sub> O <sub>3</sub>	CaO	MgO	Fe <sub>2</sub> O <sub>3</sub>	SO <sub>3</sub>
Slag	31.73	13.84	40.76	7.87	2.01	1.52
Fly ash	55.01	28.5	2.39	2.19	8.05	–

Low air-induced water-reducing agent was used which is produced by Shenyang Dongling concrete admixture company, China. It is a polycarboxylate superplasticizer with solid content of 20%. The mix proportions are shown in Table 3. The compressive strength test specimens were made of 100 mm × 100 mm × 100 mm. After curing for 24 h, the specimens were demolded and transported to the curing room for 7 and 28 days for testing. The workability and compressive strength of concrete are shown in Table 4.

**Table 3.** Mix proportions of concrete (kg/m<sup>3</sup>).

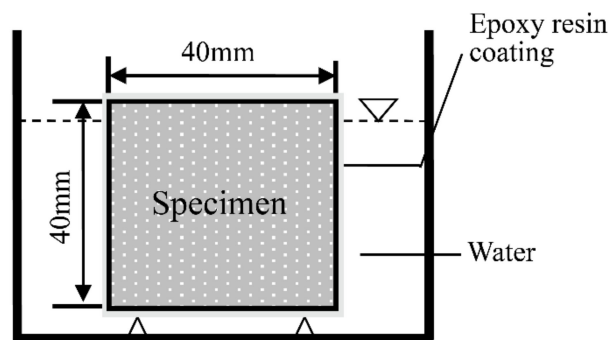
Binder Types	Water	Cement	Sand	Slag	Fly Ash	Coarse Aggregate	Water Reducing Agent
OPC	215	420	660	-	-	1264	4.5
OPC with slag	180	340	798	100	-	1264	4.5
OPC with fly ash	180	380	798	-	70	1264	4.5
OPC with slag and fly ash	180	340	798	65	35	1264	4.5

**Table 4.** Workability and compressive strength of concrete.

Binder Types	Slump/mm	Compressive Strength/MPa
OPC	225	35.9
OPC with slag	200	41.5
OPC with fly ash	250	39.1
OPC with compound admixture	230	44.7

### 3. Water Absorption Test of Concrete

Duplicate specimens (40 mm × 40 mm × 160 mm) of mortar were used to determine the water absorption values of concrete at 7 and 28 days. The specimens were dried at 105 °C to constant, and the initial weight of all specimens was recorded. Then the surface of the specimens was coated with epoxy resin, except for an exposed surface. The cured specimens were immersed in water at 20 ± 2 °C, and the water head was maintained at 2.3 cm. Then the weight of the text specimens was recorded at a specified time interval, which can be set longer as the program continues. The schematic diagram of the water absorption test is shown in Figure 1.

**Figure 1.** Schematic diagram of water absorption test.

Due to the strong barrier effect of epoxy resin, only one bottom surface can directly contact with water, which ensures the one-way transmission path of water. We all realize that only when the pores in concrete are connected with each other, the liquid will transfer freely and rapidly between the pores. Therefore, the volume of the permeable pore equals to the volume of the cumulative water absorption and the connecting porosity in one direction, which can be obtained by Equation (1).

$$\theta = m_f / (\rho_f \cdot V) \quad (1)$$

where  $\theta$  is connecting porosity,  $m_f$  is mass of fluid,  $\rho_f$  is density of water, and  $V$  is total volume of the tested specimen.

In addition, concrete is a kind of porous material, assuming that the capillary of concrete is multidimensional random parallel distribution, and the pore structure is cylindrical. The flow increment of concrete could be expressed as Equation (2) [18].

$$W(t) = n\pi r^2 \rho \sqrt{t \frac{r\gamma \cos \theta}{2\eta}} = s \sqrt{t} \tag{2}$$

where  $W(t)$  is flow increment,  $n$  is mass of pores,  $r$  is pore size,  $\rho$  is density of water,  $t$  is time,  $\gamma$  is surface tension of water,  $\theta$  is contact angle of water,  $\eta$  is viscosity of water,  $s$  is coefficient of capillary absorption.

According to the characteristics of data collection and Equation (2), generalized least squares method could be used to calculate the capillary absorption rate of concrete. Figures 2 and 3 show the experimental imbibition data (expressed as cumulative absorbed volume/unit inflow area vs.  $t_{1/2}$ ).

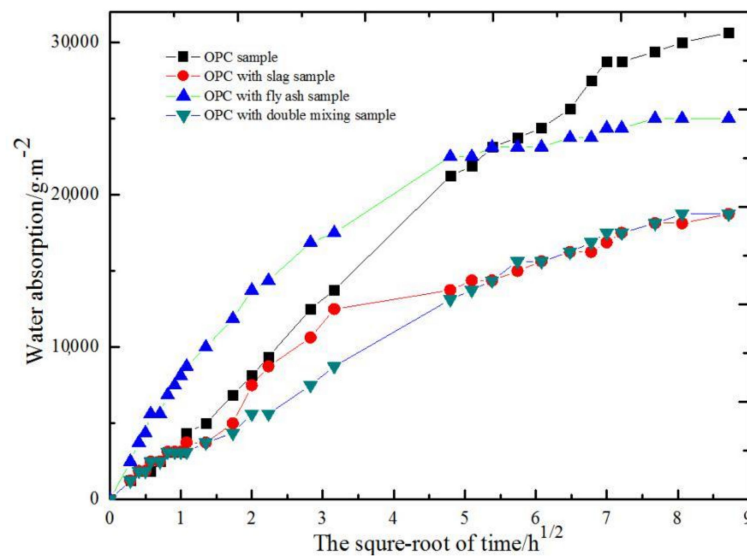


Figure 2. Relationship between water absorption and square root of time (7 days cured concrete).

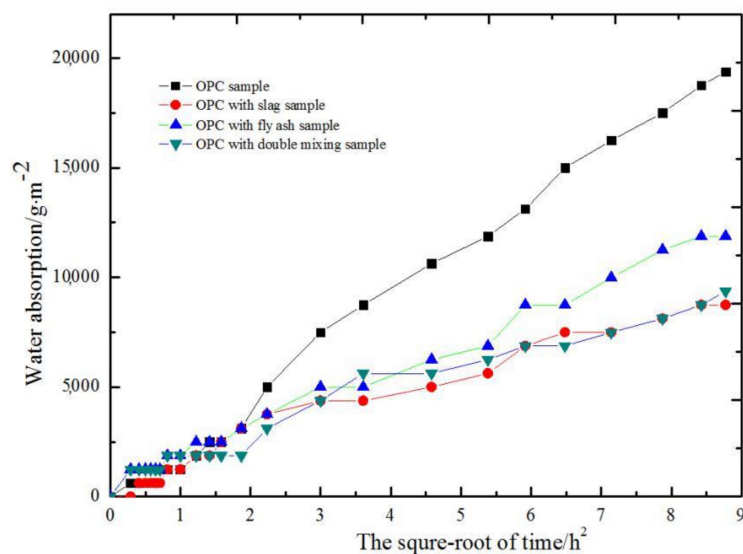


Figure 3. Relationship between water absorption and square root of time (28 days cured concrete).

As the curing time prolongs, the water absorption of all samples decreases (as shown in Figure 4). Comparison sample has the highest water absorption, followed by fly ash. Slag sample and double mixing sample have the best water absorption resistance.

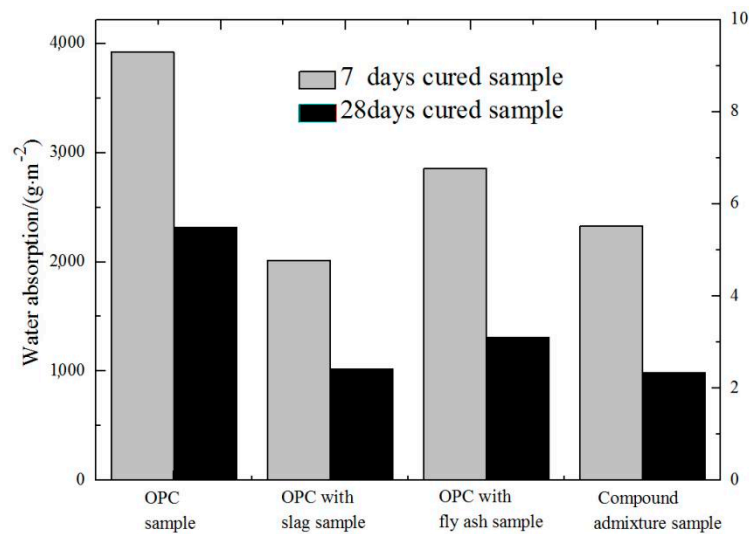


Figure 4. Water absorption of concrete.

The results show that the water absorption of concrete can be effectively reduced by adding two mineral additives (fly ash and slag), and the water absorption reduction effect of slag powder is more remarkable than that of fly ash.

#### 4. Pore Fractal Dimension

##### 4.1. MIP Test

After 28 days of standard curing, the concrete particles with the particle size of 3–5 mm were screened out by small hammer. The hydration reaction in the concrete particles was terminated by anhydrous ethanol. The treated samples were put into the oven and dried continuously at  $105 \pm 2$  °C for 6 h to remove the excess moisture. The samples were put into the dilatometer and tested by mercury intrusion method.

In addition, samples were placed in an oven at 105 °C for 6 h to remove residual water or alcohol. Finally, the micropore structure was investigated using mercury intrusion porosimetry (MIP). The mercury injection test results of the four kinds of concrete after curing 28 d are shown in Figures 5 and 6.

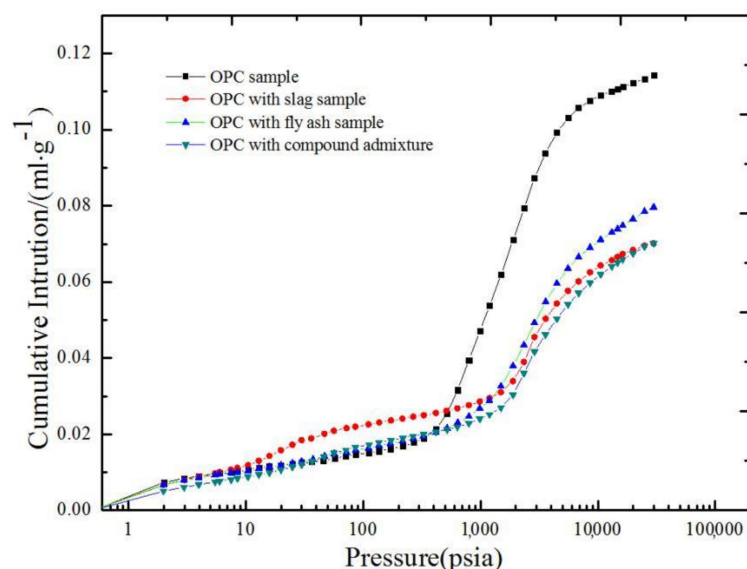
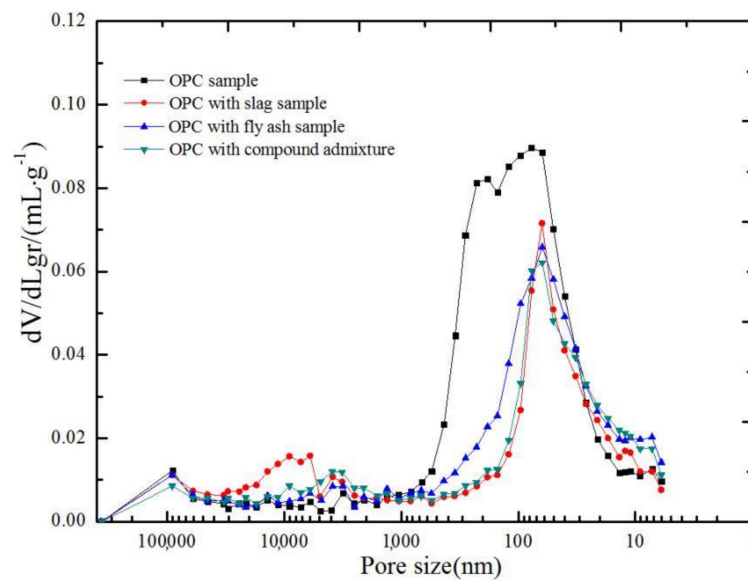
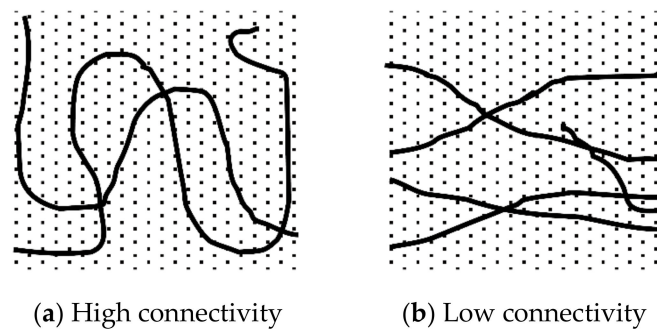


Figure 5. MIP curves of relationship between pressure and cumulative intrusion.



**Figure 6.** Pore size distribution of cement mortar.

Besides, connecting porosity as a one-dimension value of concrete, the proportion of the connecting porosity ( $\theta$ ) in total porosity ( $\theta_T$ ) of concrete can be seen as the connectivity probability among pores on a specific rotation direction. The schematic drawing of the pores distributing in concrete is shown in Figure 7.



**Figure 7.** Schematic drawing of the different connectivity probability.

It can be seen that the pore is intricately distributed in concrete, and their connection behavior occurs naturally and randomly. The permeability of porous concrete in different states under the same pore conditions is obviously different. Porosity has a direct physical meaning (void volume ratio), tortuosity is either an indirect or inferred measure of how the flow rate is affected (by twists and turns) within the porous medium. Highly interconnected connectivity as mentioned in the paper, is low tortuosity.

Therefore, the ratio ( $\theta/\theta_T$ ) can be used to describe the connectivity trend in pore formation process. According to the data collected by MIP, the pore size distributions and connectivity probability ( $\theta/\theta_T$ ) are shown in Table 5.

**Table 5.** Pore size distribution and connectivity probability of concrete.

Binder Types	Porosity/%				Total Porosity/%	Connectivity Probability/%
	>10 <sup>3</sup> nm	10 <sup>3</sup> –10 <sup>2</sup> nm	10 <sup>2</sup> –10 nm	<10 nm		
OPC	14.34	46.40	37.14	2.12	21.54	56.22
OPC with slag	33.82	13.82	49.20	3.17	14.78	37.01
OPC with fly ash	22.20	24.20	48.69	4.91	16.13	46.00
OPC with compound admixture	26.42	16.07	52.79	4.72	13.48	43.47

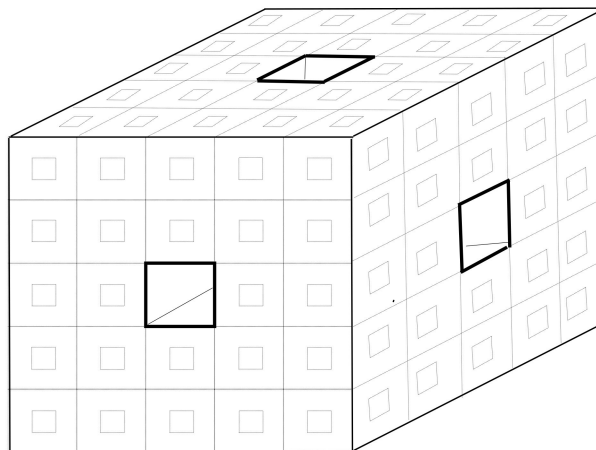
#### 4.2. Calculation of Pore Fractal Dimension

Based on the fractal theory and the related micropore model, the deep information in concrete can be revealed. The Menger sponge model (shown in Figure 8) is an optimal fractal structure, which can be used to simulate the complex state of pore distribution in concrete [19]. The fractal model is established to simulate the fractal pores of materials. The cube with side length  $R$  is divided into equal-sized small cubes. We selected a rule, removed some of these small cubes, and the remaining small cubes were  $N(m)$ . With this operation, the size of the remaining cubes decreases and the number increases. The remaining infinitely small cubes form the matrix of the material, while the small cube spaces with different orders are removed to form the pores of different orders in the material. After  $k$  operations, the remaining cube size is  $r_k = R/m_k$ . The following equations can be obtained:

$$N_k = (r_k/R)^{-D} \quad (3)$$

where  $D$  is dimension of pore volume, and the structure volume can be deduced as follows:

$$V_k \propto r_k^{3-D} \quad (4)$$

**Figure 8.** Menger sponge model.

According to Equation (4) and the relation between pressure and pore size, the  $dV$  and  $dr$  are taken as logarithmic, respectively, to draw the curve, the fractal dimension of porous volume can be determined by the slope of the curve.  $\text{Lgr}$  and  $\text{Lg}V$  are the logarithm to  $r$  and the logarithm to  $V$ , respectively. The relationship between  $\text{Lgr}$  and  $\text{Lg}V$  are shown in Figures 9–12.

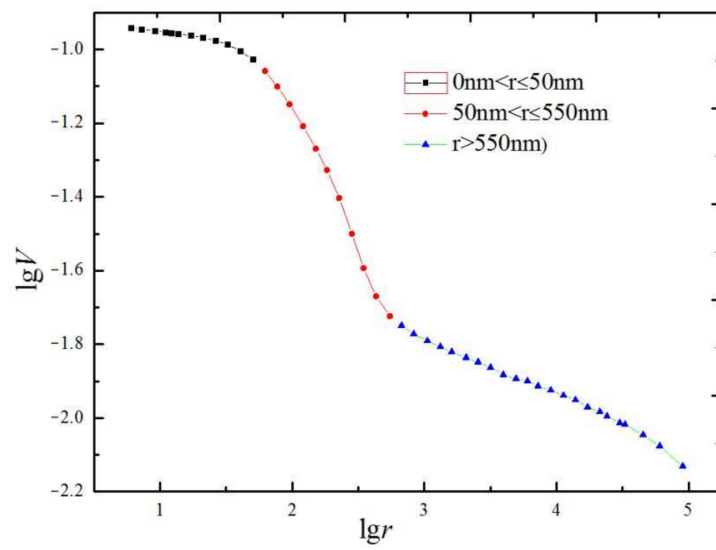


Figure 9. Relationship between Lgr and LgV of comparing concrete.

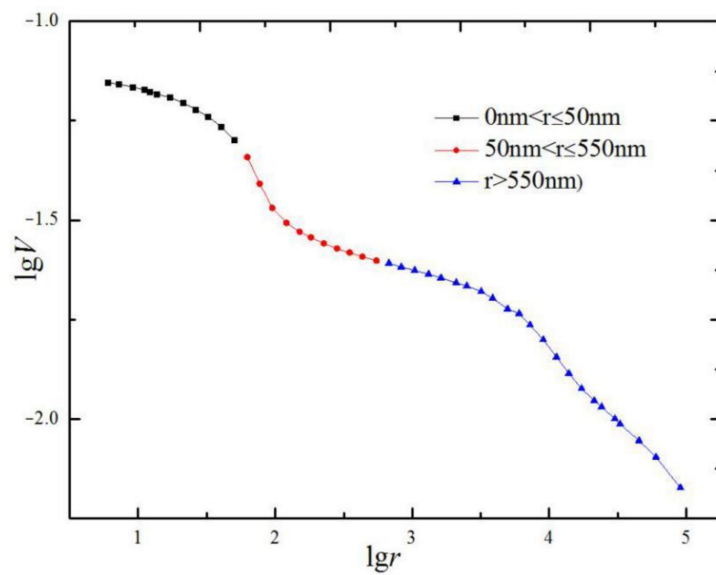


Figure 10. Relationship between Lgr and LgV of slag concrete.

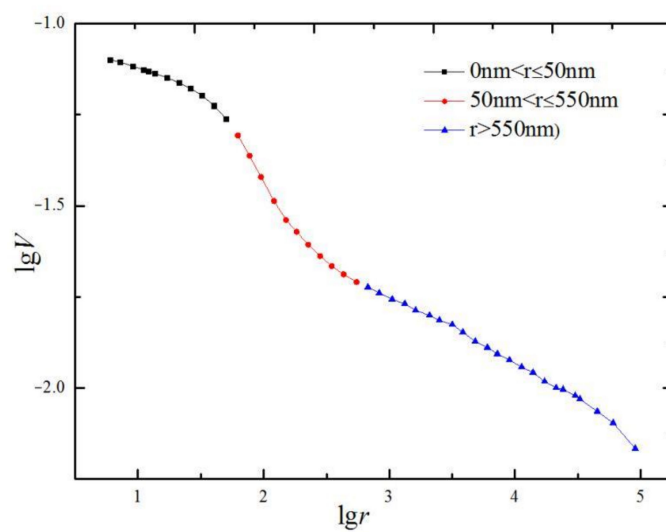
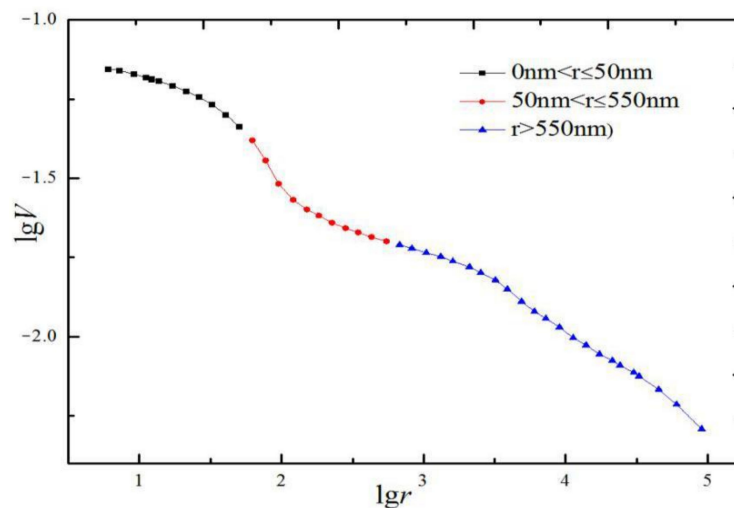


Figure 11. Relationship between Lgr and LgV of fly ash concrete.



**Figure 12.** Relationship between  $Lgr$  and  $LgV$  of OPC with compound admixture.

The above figure shows that there are inflection points near the aperture of 50 and 550 nm, so the relationship between  $Lgr$  and  $LgV$  cannot be described as a straight line, but two straight lines. In fact, when trying to establish a relationship between fractal values and macroscopic properties, the polytrope of fractal dimension should be taken into consideration among different size scope, because it turns out to be different fractal properties with different size scope of an object, then the fractal dimension of pores in concrete should be achieved segmentally by the relationship according to Equation (4), and the pore fractal volume dimension obtained through the calculation of mercury intrusion data are shown in Table 6.

**Table 6.** Fractal dimension of pores and correlation coefficients.

		$d_1$ (<50 nm)	$d_2$ (50~550 nm)	$d_3$ (>550 nm)	$d$
OPC	$D$	2.9188	2.2584	2.8394	2.6651
	$R$	0.9432	0.9933	0.9947	0.9677
OPC with slag	$D$	2.8525	2.7553	2.7269	2.7693
	$R$	0.9632	0.8289	0.9762	0.9856
OPC with fly ash	$D$	2.8367	2.5721	2.8042	2.7327
	$R$	0.9722	0.9822	0.9954	0.9843
OPC with compound admixture	$D$	2.8118	2.6849	2.7244	2.7308
	$R$	0.9730	0.9473	0.9919	0.9939

## 5. Results and Discussion

The investigations performed in this study showed that alterations of mineral admixture can seriously affect the water absorption of concrete as is shown in Figure 13. Alterations of mineral admixture are not limited to macroscopic effect but act in the microstructure evolution of concrete. Mineral admixtures could refine the pore structures indeed, which is quantified as fractal dimension in this paper. Additionally, thinking about pore volume distribution from the perspective of the ideal fractal model, higher pore volume dimension means more complex pores distributed in concrete, under the same porosity conditions. The more complex the pore is, the longer the transmission path of water is, and also the transportation time which makes it a lower water absorption value of concrete [20]. Due to these assumptions, total pore fractal dimension should have a good agreement with water absorption value. The relation between water absorption values and total pore dimension is as shown below:

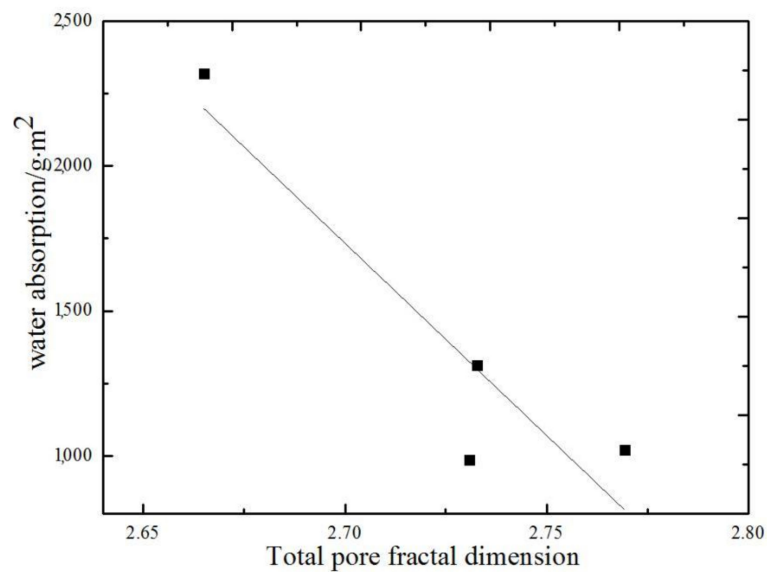


**Figure 13.** Relationship between water absorption values and total pore dimension (28 days cured concrete).

However, this is not an ideal case. As shown in Figure 13, there is no good correlation between the total pore volume size and the water absorption value (correlation coefficient is 0.78). Especially when the fractal dimension is 2.7308 and 2.7327, the water absorption rate is higher with the increase of the fractal dimension. It is concluded that the fractal dimension of total pore volume does contain all the information of the complex state of pores. In Figures 9–12, there are inflection points in the relationship curve between  $Lgr$  and  $LgV$ . Therefore, the total pore fractal dimension cannot accurately reflect the complex state of the pore. Therefore, the key factor to establish the objective relationship between pore complexity and water absorption value is to select the appropriate section of pore size, accurately characterize its complexity by pore fractal dimension, and explain the most possible pore size of concrete. The relationship of water absorption value and fractal dimension of 50~550 nm is shown in Figures 14 and 15.

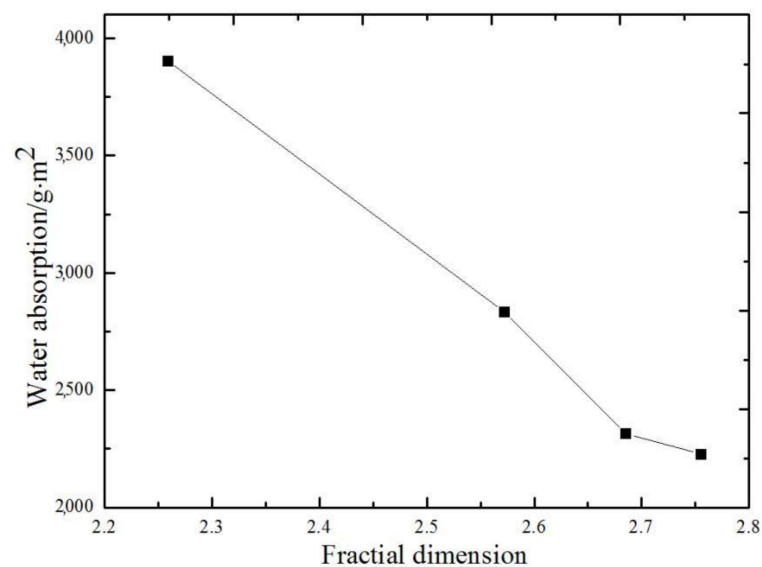


**Figure 14.** Relationship of water absorption value and fractal dimension of 50~550 nm (7 days cured concrete).

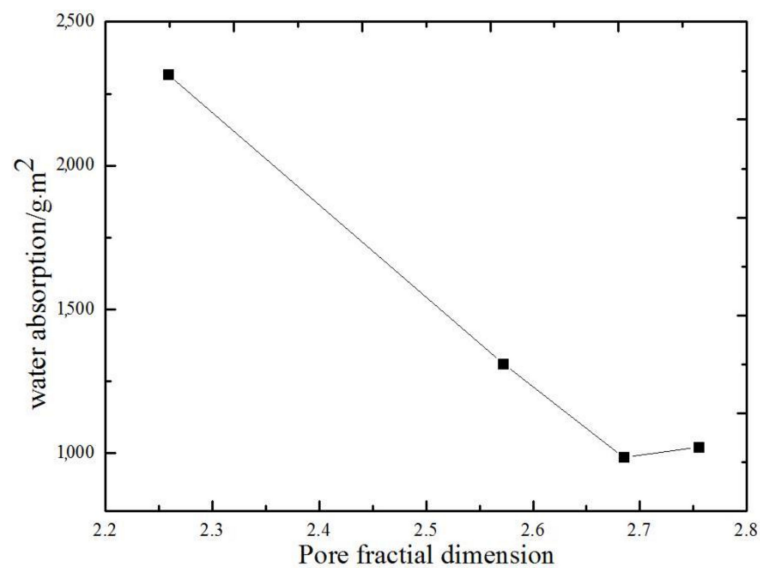


**Figure 15.** Relationship of water absorption value and fractal dimension of 50~550 nm (28 days cured concrete).

The fractal dimension of the comparing sample is obviously higher than that of the other samples with a most probable aperture near 671 nm. From another point of view, it is concluded that the fractal dimension of pore size of the comparing sample is the lowest between 50 and 550 nm, so there is another most possible pore size between 50 and 550 nm. From the mercury injection data, it can be seen the results of this analysis. Therefore, due to the inherent defects of MIP (high pressure, solid particle breakage, etc.), all samples have the maximum possible pore size between 50 and 550 nm. Compared with other sections, the middle section of pore diameter can always accurately describe the complex state of the pore, so that the fractal dimension of the pore between 50 and 550 nm has a good linear relationship with the water absorption value. The correlation coefficients of concrete cured on 7 and 28 d are greater than 0.95. Although the samples were tested at 28 days, there was a significant correlation between the absorption value of 7 days and the fractal volume dimension. The results show that the pore volume fractal dimension of 50–550 nm can be used to evaluate the water absorption of concrete. Furthermore, the pores with small fractal dimension correspond to low complexity of pores, which indicates that the pore tends to be simplified. Therefore, with the increase of pore fractal dimension, the probability of pore connectivity decreases. The relationship between connectivity probability of pores and pore volume dimension of 50~550 nm is shown in Figure 16.

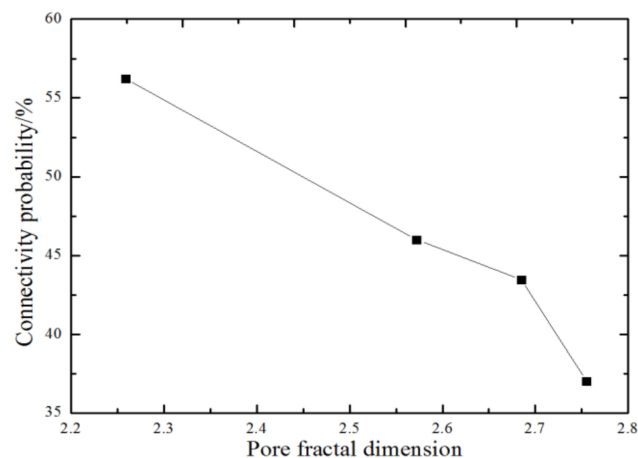


**Figure 16.** Relationship between connectivity probability of pores and pore volume dimension of 50~550 nm.

As shown in the figure above, the fractal dimension of pores in concrete is closely related to the probability of pore connectivity, and the correlation coefficient can reach 0.935. The above correlation can be explained by the quantification of pore fractal dimension between 50 and 550 nm, which quantifies the complexity of internal pores in concrete. The discovery of the relationship between fractal dimension and probability of pores distribution plays an important role in studying the internal possibility of concrete with the theory of chaos and fractal.

## 6. Conclusions

- (1) The pore structure of different regions shows different fractal characteristics. Fractal theory can analyze and evaluate the pore structure characteristics of concrete, especially when evaluating the permeability of concrete, the complexity of pore structure can be described in detail and quantitatively.
- (2) With the extension of curing time, the water absorption value of all samples will decrease. Adding two mineral additives (fly ash and slag) can effectively reduce the water absorption of concrete, and the water absorption reduction effect of slag powder is more significant than that of fly ash.
- (3) Compared with the total pore fractal dimension, the pore fractal dimension of 50–550 nm can accurately describe the complex state of the pore, and the pore fractal dimension of 50–550 nm has a good linear relationship with the water absorption value.
- (4) Pore fractal dimension between 50 and 550 nm has a close correlation with connectivity probability of pores inside concrete. The fractal theory could be applied for researching the probability of pore distribution inside concrete. The pore fractal dimension of 50–550 nm is closely related to the probability of pore connectivity in concrete. Fractal theory can be used to study the internal probability of concrete.

**Author Contributions:** Conceptualization, X.D. and J.Z.; methodology, X.D.; software, T.K.; validation, Y.Z., Y.F. and T.K.; formal analysis, Y.Z.; investigation, Y.Z.; resources, Y.Z.; data curation, T.K.; writing—original draft preparation, Y.Z. and X.L.; writing—review and editing, Y.F.; visualization, Y.F.; supervision, J.Z.; project administration, J.Z.; funding acquisition, J.Z. All authors have read and agreed to the published version of the manuscript.

**Funding:** This work was financially supported by the National Natural Science Foundation of China (51678374), the Liaoning Province Natural Science Foundation of China (20180550092), the Innovation Team Project of Liaoning (LT2019011) State Key Laboratory of Silicate Materials for Architectures (SYSJJ2020-15).

**Acknowledgments:** Special thanks are extended anonymous reviewers for their value comments.

**Conflicts of Interest:** The authors declare no conflict of interest.

## References

1. Neville, A. Consideration of durability of concrete structures: Past, present, and future. *Mater. Struct.* **2001**, *34*, 114–118. [[CrossRef](#)]
2. Basheer, L.; Cleland, D.J. Durability and water absorption properties of surface treated concretes. *Mater. Struct.* **2011**, *44*, 957–967. [[CrossRef](#)]
3. Juenger, M.C.G.; Siddique, R. Recent advances in understanding the role of supplementary cementitious materials in concrete. *Cem. Concr. Res.* **2015**, *78*, 71–80. [[CrossRef](#)]
4. Bremner, T.; Hover, K.; Poston, R.; Broomfield, J.; Joseph, T.; Price, R.; Clear, K.; Khan, M.; Reddy, D.; Clifton, J. *ACI 222R-01 Protection of Metals in Concrete Against Corrosion*; American Concrete Institute: Farmington Hills, MI, USA, 2001.
5. Li, K.; Li, C. Modeling hydroionic transport in cement-based porous materials under drying-wetting actions. *J. Appl. Mech.* **2013**, *80*, 20904. [[CrossRef](#)]
6. Bassuoni, M.T.; Nehdi, M.L. Durability of self-consolidating concrete to different exposure regimes of sodium sulfate attack. *Mater. Struct.* **2009**, *42*, 1039–1057. [[CrossRef](#)]

7. Zhao, X.-l.; Wei, J.; Liu, Z.-k. Durability of concrete under multi-damage action. *J. Wuhan Univ. Technol. Mater. Sci. Ed.* **2004**, *19*, 73–75. [[CrossRef](#)]
8. Safiuddin, M.; Mahmud, H.B.; Jumaat, M.Z. Efficacy of ASTM saturation techniques for measuring the water absorption of concrete. *Arab. J. Sci. Eng.* **2011**, *36*, 761. [[CrossRef](#)]
9. Khan, M.I.; Mourad, S.M.; Charif, A. Utilization of supplementary cementitious materials in HPC: From rheology to pore structure. *KSCE J. Civ. Eng.* **2017**, *21*, 889–899. [[CrossRef](#)]
10. Tang, M.; Li, X. Current situation and development of concrete fractal characteristic. *Concrete* **2004**, *12*, 8–11. [[CrossRef](#)]
11. Dubuc, B.; Quiniou, J.F.; Roques, C.C.; Tricot, C.; Zucker, S.W. Evaluating the fractal dimension of profiles. *Phys. Rev. A* **1989**, *39*, 1500–1512. [[CrossRef](#)] [[PubMed](#)]
12. Guo, W.; Qin, H.; Chen, H.; Sun, W. Fractal theory and its applications in the study of concrete materials. *J. Chin. Ceram. Soc.* **2010**, *38*, 1362–1368.
13. Tang, M.; Chen, Z.; Yang, F. Research on characteristics of pore fractal and chloride diffusion in C50 pumped concrete. *Concrete* **2010**, 92–95. [[CrossRef](#)]
14. Yin, H.; Lv, H.; Zhao, Y. Fractal characteristics of cement paste by carbonation. *Concrete* **2009**, 97–99. [[CrossRef](#)]
15. Jin, S.; Zhang, J.; Huang, B. The relationship between freeze-thaw resistance and pore structure of concrete. *Pavement Geotech. Eng. Transp.* **2013**, 60–67. [[CrossRef](#)]
16. Chen, X.; Zhou, J.; Ding, N. Fractal characterization of pore system evolution in cementitious materials. *KSCE J. Civ. Eng.* **2015**, *19*, 719–724. [[CrossRef](#)]
17. Xue, S.; Zhang, P.; Bao, j.; He, L.; Hu, Y.; Yang, S. Comparison of Mercury Intrusion Porosimetry and multi-scale X-ray CT on characterizing the microstructure of heat-treated cement mortar. *Mater. Charact.* **2020**, *160*, 110085. [[CrossRef](#)]
18. Gummerson, R.J.; Hall, C.; Hoff, W.D. Water movement in porous building materials—II. Hydraulic suction and sorptivity of brick and other masonry materials. *Build. Environ.* **1980**, *15*, 101–108. [[CrossRef](#)]
19. Tang, M.; Wang, J.; Li, L. Research on fractal characteristics of concrete materials pore with MIP. *J. Shenyang Archit. Civ. Eng. Inst.* **2001**, *17*, 272–275. [[CrossRef](#)]
20. Xie, C.; Wang, Q.; Li, S.; Hui, B. Relations of pore fractal dimension to pore structure and compressive strength of concrete under different water to binder ratio and curing condition. *Bull. Chin. Ceram. Soc.* **2015**, *34*, 3695–3702.



© 2020 by the authors. Licensee MDPI, Basel, Switzerland. This article is an open access article distributed under the terms and conditions of the Creative Commons Attribution (CC BY) license (<http://creativecommons.org/licenses/by/4.0/>).